Short communication

An investigation of jogging biomechanics using the full-body lumbar spine model: Model development and validation

Margaret E. Raabe *, Ajit M.W. Chaudhari

ª Department of Biomedical Engineering, The Ohio State University, 2050 Kenny Rd, Suite 3100, Columbus, OH 43221, USA
ᵇ School of Health and Rehabilitation Sciences & Departments of Orthopaedic Surgery, Biomedical Engineering and Mechanical & Aerospace Engineering, The Ohio State University, Columbus, OH, USA

ABSTRACT

The ability of a biomechanical simulation to produce results that can translate to real-life situations is largely dependent on the physiological accuracy of the musculoskeletal model. There are a limited number of freely-available, full-body models that exist in OpenSim, and those that do exist are very limited in terms of trunk musculature and degrees of freedom in the spine. Properly modeling the motion and musculature of the trunk is necessary to most accurately estimate lower extremity and spinal loading. The objective of this study was to develop and validate a more physiologically accurate OpenSim full-body model. By building upon three previously developed OpenSim models, the full-body lumbar spine (FBLS) model, comprised of 21 segments, 30 degrees-of-freedom, and 324 musculotendon actuators, was developed. The five lumbar vertebrae were modeled as individual bodies, and coupled constraints were implemented to describe the net motion of the spine. The eight major muscle groups of the lumbar spine were modeled (rectus abdominis, external and internal obliques, erector spinae, multifidus, quadratus lumborum, psoas major, and latissimus dorsi), and many of these muscle groups were modeled as multiple fascicles allowing the large muscles to act in multiple directions. The resulting FBLS model's trunk muscle geometry, maximal isometric joint moments, and simulated muscle activations compare well to experimental data. The FBLS model will be made freely available (https://simtk.org/home/fullbodylumbar) for others to perform additional analyses and develop simulations investigating full-body dynamics and contributions of the trunk muscles to dynamic tasks.

© 2016 Published by Elsevier Ltd.

1. Introduction

Dynamic simulations of human movement are a beneficial addition to experimental data, as they enable researchers to conduct biomechanical investigations involving parameters of the neuromusculoskeletal system that are difficult or impossible to examine using experiments alone. However, the ability of a simulation's results to translate to real-life situations is dependent on the physiological accuracy of the musculoskeletal model.

OpenSim is a freely available, open-source musculoskeletal modeling software (Delp et al., 2007) that allows users to develop and analyze dynamic simulations of human movement. The open-source nature of the software results in a large database of previously built, validated, and tested musculoskeletal models for other users to expand upon. Despite this large database, very few full-body models exist in OpenSim, and those that do exist are very limited in terms of trunk musculature and degrees of freedom in the spine (Caruthers et al., 2013; Hamner et al., 2010).

Proper modeling of trunk motion and muscle activations is necessary to accurately estimate lower extremity loads as well as spinal loads. Additionally, a physiologically relevant trunk is necessary to investigate the role of core strength and stability in dynamic movements, a topic that has received increasing clinical and scientific interest over the past decade (Chaudhari et al., 2012; Ferber et al., 2015; Jamison et al., 2013; Kibler et al., 2006; McGill, 2010; Willson et al., 2005). The purpose of this study was to develop and validate a more physiologically accurate OpenSim full-body model with extensive trunk musculature and degrees of freedom in the lumbar spine.

2. Methods

2.1. Model development

The full-body lumbar spine (FBLS) model (Fig. 1) was developed by combining three previously built OpenSim models: Hamner's full-body model (Hamner et al., 2010) for the base model, Christophy's lumbar spine model (Christophy et al., 2012) for the torso, and Arnold's model (Arnold et al., 2010) of the patella. Brief details about model development will be presented here and more details can be found in the Supplemental material Section 1.1.

* Corresponding author. Tel.: +1 614 293 2246; fax: +1 614 293 2910.
E-mail address: margaret.e.raabe@gmail.com (M.E. Raabe).
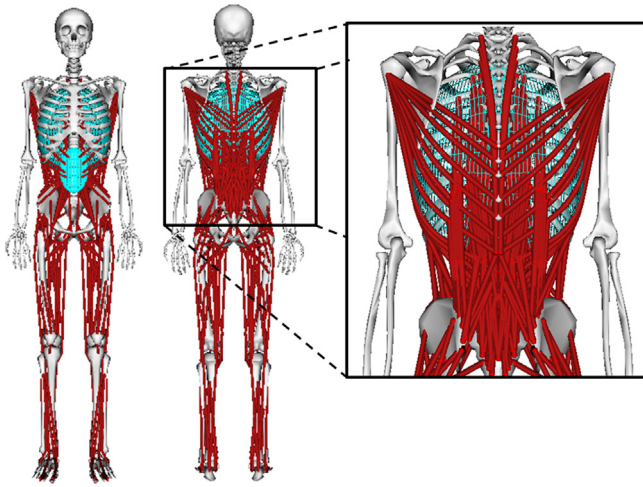
Fig. 1. The full-body lumbar spine (FBLS) model. The model consists of 324 musculotendon actuators and wrapping surfaces.

When combining the models together, extreme care was taken to ensure all models were scaled to the same size person, so that when they were combined all mass and inertial properties would be consistent across the models. After scaling the component models, discrepancies still remained since Hamner's model and Christophy's model used different ribcage and pelvis geometry. Consequently, all attachment points of the 224 trunk muscle fascicles to the ribcage and pelvis had to be adjusted to their appropriate physiological locations in the FBLS model. It was important that these were attached with close inspection to ensure the most anatomically correct muscle paths were chosen, because incorrect attachments and paths would result in non-physiological estimations of muscle activations and forces.

The resulting FBLS model is comprised of 21 segments, 30 degrees-of-freedom, and 324 musculotendon actuators. The five lumbar vertebrae are modeled as individual bodies, each connected by a 6 degree-of-freedom joint (Christophy et al., 2012). After 27 coupling constraints are imposed, the net lumbar movement is described as three rotational degrees-of-freedom: flexion-extension, lateral bending, and axial rotation (Christophy et al., 2012). The rigid torso (lumped thoracic and cervical vertebrae, ribcage, scapulae, and head) is connected to the first lumbar vertebrae by a one degree-of-freedom rotational joint that allows for additional axial rotation of the torso, if necessary. While some detailed musculoskeletal models of the spine exist (Bruno et al., 2015; Christophy et al., 2012; de Zee et al., 2007), the FBLS model is the first full-body OpenSim model to describe the trunk musculature in this level of detail. The eight major muscle groups of the lumbar spine that are modeled include the erector spinae (ES), rectus abdominis (RA), external obliques (EO), internal obliques (IO), multifidus (MF), quadratus lumborum (QL), psoas major (PS), and latissimus dorsi (LD). Every muscle group is modeled as multiple fascicles with different lines of action to account for the fact that most of the trunk muscles are large and can act in multiple directions (Christophy et al., 2012). The ES is defined as the iliocostalis lumborum (IL) and the longissimus thoracis (LT), each of which have a rib/thoracic (IL_R, LTpT) and lumbar component (IL_L, LTpL). Wrapping surfaces are also included in the model to ensure physiological muscle lines of action.

2.2. Model validation

The model validation process includes comparing model parameters and simulations to experimental data to ensure that they represent the physical phenomena of interest (Hicks et al., 2015). We validated the FBLS model through the three phases described in the following sections that have previously been used to validate the capability of a musculoskeletal model to produce a dynamic simulation (Arnold et al., 2010; Hicks et al., 2015; Holzbaur et al., 2005).

2.2.1. Validating model parameters

The first step of the validation process is to validate model parameters by comparing them to experimental values measured *in vivo* or in cadavers. Authors of the three individual models have each done extensive literature research to determine the individual segment and muscle properties of their models and very few of these were altered when developing the FBLS model. The only individual muscle parameter altered in development of this model was the maximum isometric force property in several of the trunk and lower extremity muscles that were found to be too weak for simulations of jogging (listed in Supplemental Table 1). As mentioned previously, since several of the trunk muscle attachment points were altered it was necessary to validate the trunk muscle geometry to ensure that muscle attachments and lines of action were physiologically relevant. To do this, we compared the trunk muscle sagittal plane moment arms at zero degrees trunk flexion to those measured experimentally in the literature (Jorgensen et al., 2001).

2.2.2. Validating muscle function

Next, we validated muscle function by examining the model's moment generating capacity about a given joint to ensure the moment is comparable to experimental results. For more details on how OpenSim calculates maximum isometric joint moments, see the Supplemental material Section 1.3. Since minimal changes were made to the lower extremities during development of this model, validation was focused on the function of the trunk musculature about the L5-S1 joint.

Maximal isometric trunk joint moments measured experimentally in our laboratory and similar data reported in the literature were compared to the moment generating capacity of our model. Seven healthy adult males (mass = 79.30 ± 9.18 kg, height = 1.79 ± 0.07 m, age = 22.43 ± 2.89 y) participated after providing IRB-approved consent. To experimentally measure the trunk flexion, extension, and lateral bending moments a custom device described elsewhere was used (Jamison et al., 2012). For more information on this testing process, see the Supplemental material Section 1.4.

2.2.3. Validating simulations

Lastly, model simulations were validated by comparing model muscle activations estimated during Static Optimization to experimentally measured surface electromyography (EMG) during overground jogging at a comfortable speed (2.48 ± 0.25 m/s). Kinematics, kinetics, and EMG during jogging were collected for one healthy participant (male, mass = 100.93 kg, height = 1.85 m, age = 30 y) as part of another IRB-approved study. The generic musculoskeletal model was scaled to match the anthropometry of the study participant. Inverse Kinematics, Inverse Dynamics (using the residual reduction algorithm), and Static Optimization (SO) were performed in OpenSim (Delp et al., 2007) to estimate individual muscle activations during jogging. Surface electromyography (EMG) was performed on the following muscles as described by McGill et al. (1996) or directly on the muscle belly unilaterally on the dominant side (bilaterally for obliques): RA, EO, IO, erector spinae (L5), gluteus maximus (GMax), gluteus medius (GMed), rectus femoris (RF), vastus lateralis (VL), vastus medialis (VM), biceps femoris (BF), semitendinosus (ST), lateral gastrocnemius (LG), soleus (Sol), and tibialis anterior (TA). Before analysis, EMG was processed (10–500 Hz band-pass filtered, rectified, and RMS smoothed with 60 ms window) and normalized to the peak activation over the gait cycle. A 40 ms delay was applied to processed EMG to account for electromechanical delay between surface EMG and force production (Arnold et al., 2013). Normalized EMG was compared to simulated muscle activations, which are defined between 0 and 1. For muscle groups that are modeled as multiple fascicles, we compared the average activation of all the fascicles in the muscle group to the corresponding EMG.

3. Results and discussion

3.1. Model parameters

Sagittal plane moment arms for the RA, EO, and IO muscle fascicles with respect to each of the lumbar vertebral levels are shown in Table 1. The moment arm of each fascicle and the average (AVG) moment arm for a group of muscle fascicles was compared to the moment arm for the respective muscle group recorded by Jorgensen et al. (2001) experimentally using magnetic resonance imaging. It is important to note that often, one experimentally measured moment arm for an entire muscle group is compared to all of the individual fascicles for that muscle group in the model. The RA, EO, and IO muscle groups were found to have fascicles with a moment arm within one SD of the experimentally collected moment arm for almost all joint levels. The FBLS model was scaled to the average height and weight of the subjects for which experimental data was collected (Jorgensen et al., 2001); however, ribcage geometry and spinal curvature of the model were not subject specific. Additionally, if multiple fascicles in a muscle group crossed a given joint level, it was unknown for which of these fascicles experimental data was collected. These limitations may explain why model moment arms compare well to experimental data at certain joint levels but not as well at others. This same analysis was completed for all trunk muscle fascicles (Supplemental Table 2) and similar results were found.

3.2. Muscle function

Fig. 2 shows maximum isometric joint moments for the trunk degrees-of-freedom in the model compared to the experimental

data collected in this study and data in the literature examining trunk strength at multiple joint angles (Keller and Roy, 2002; Khalaf et al., 1997; Kumar et al., 1995). While the model's joint moments do not correspond exactly with experimental data, the general behavior is comparable. These differences between the model and experimental data may arise due to slight differences between muscle physiological cross sectional area and tendon slack length parameters in the model and in the population for which experimental data was collected. These values in the model are generally acquired through cadaveric studies, which may not be representative of a young, healthy experimental population. The maximum isometric force properties for several muscles have

Table 1
Sagittal plane moment arms for RA, EO, and IO muscle fascicles.

| Fascicle | Moment arm (mm) with respect to given lumbar vertebral joint level | | | | |
	L1-L2	L2-L3	L3-L4	L4-L5	L5-S1
Rectus abdominis					
RA	73^ ^	76^ ^	64^ ^	64*	75*
External oblique					
EO1	74*	85^ ^	85^ ^	90^ ^	40*
EO2	70*	80^ ^	81^ ^	87^ ^	37*
EO3	55**	67**	70^ ^	80^ ^	36*
EO4	41^ ^	54*	61^ ^	73^ ^	34*
EO5	7^ ^	10^ ^	14*	25*	45*
EO6	6^ ^	4^ ^	2^	15*	36*
AVG	42˜	50*	52^	62^ ^	38*
Internal oblique					
IO1	N/A	N/A	N/A	N/A	37*
IO2	N/A	N/A	N/A	N/A	30**
IO3	N/A	N/A	N/A	N/A	36*
IO4	57^ ^	53^	39*	31*	20^
IO5	28^ ^	22^ ^	12^ ^	8^	16˜
IO6	1^ ^	5^ ^	10^ ^	7^	6^ ^
AVG	29^ ^	27^ ^	20^	16**	24^

A *,**,^ or ^^ signifies the model's moment arm was within 1 standard deviation (SD), 1.01–1.5 SD, 1.51–2 SD, or 2.01+ SD, respectively, of Jorgensen et al.'s experimentally collected data Jorgensen Jorgensen et al. (2001).
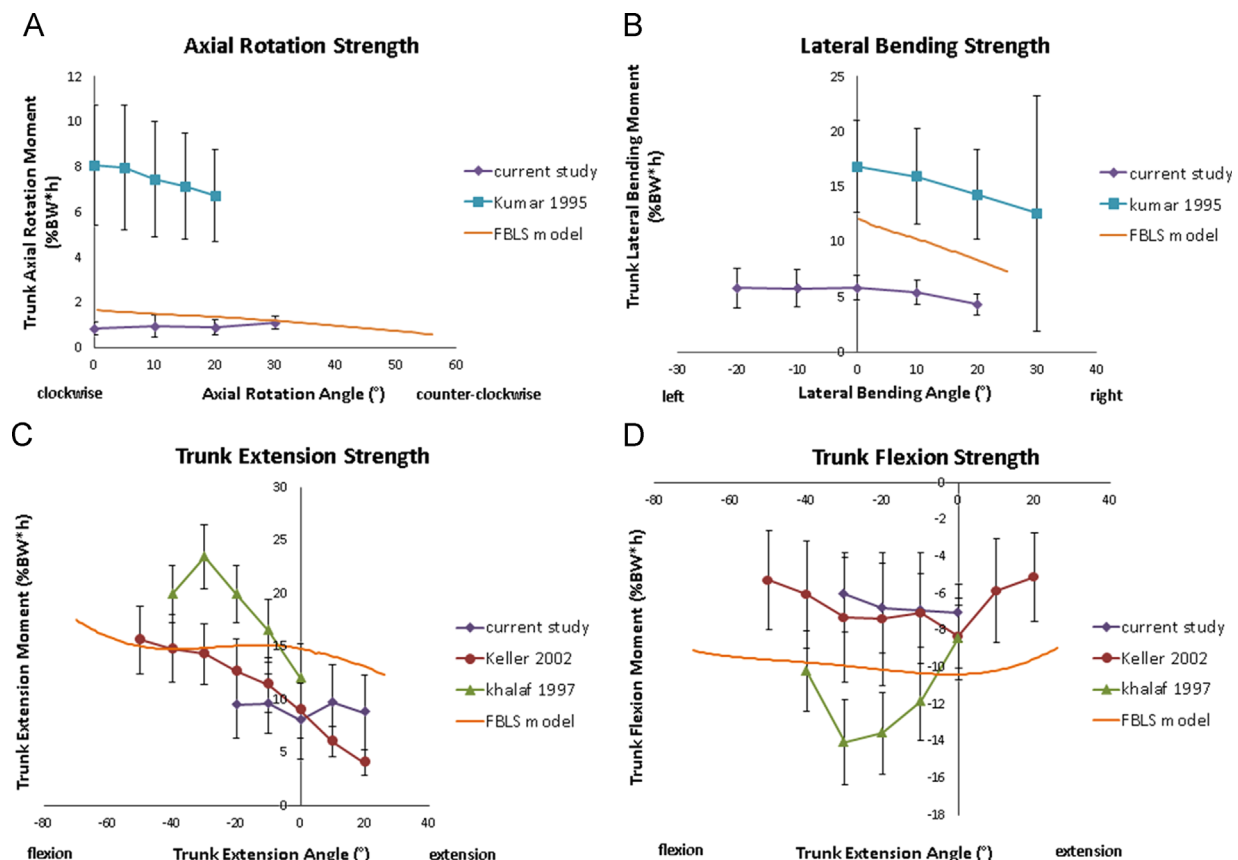
Fig. 2. Maximum isometric joint moments for axial rotation (A), lateral bending (B), trunk extension (C), and trunk flexion (D) in the model compared to experimental data collected in this study and data in the literature examining trunk strength at multiple joint angles.
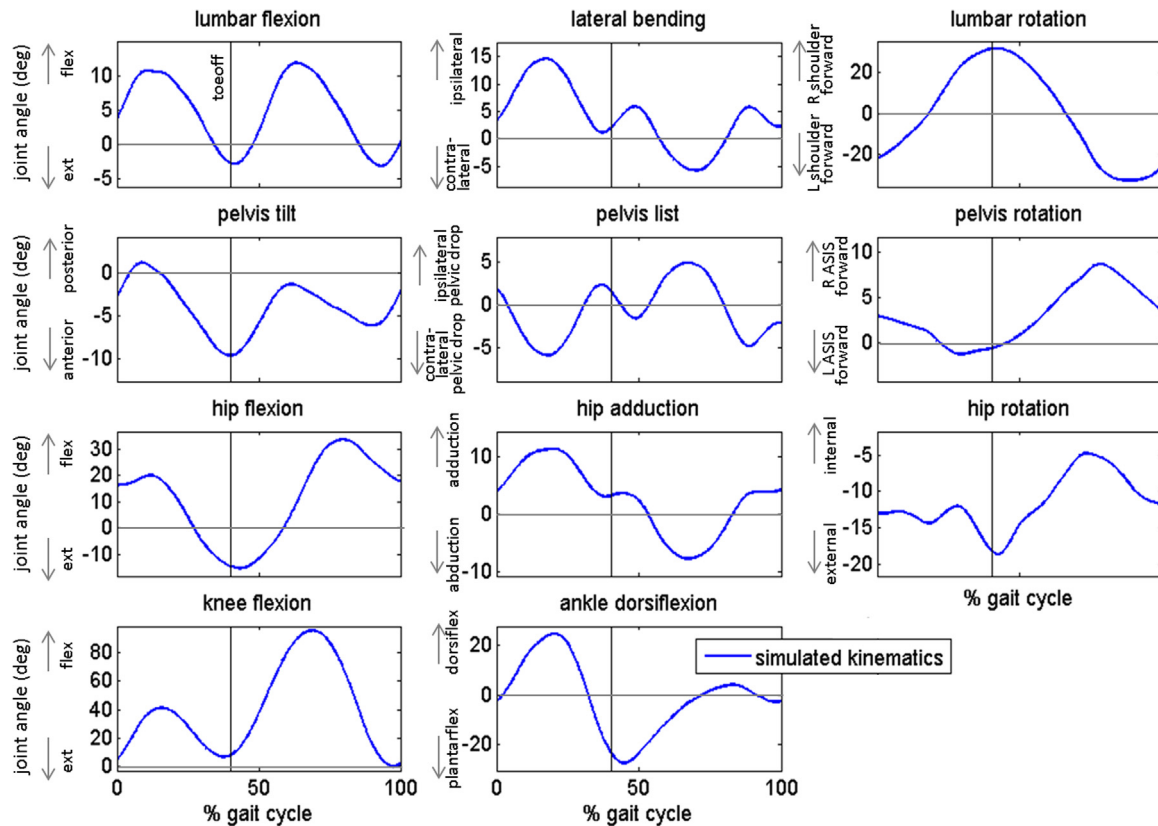
Fig. 3. Trunk and lower extremity jogging kinematics simulated using the FBLS model over one right foot gait cycle. Abbreviations: right (R) or left (L) anterior superior iliac spine (ASIS), extension (ext), flexion (flex), plantarflexion (plantarflex), dorsiflexion (dorsiflex). The direction of lateral bending and pelvis list is with reference to the stance leg.

been scaled up to account for this difference, but this will not account for all discrepancies.

Additionally, when calculating the maximum isometric joint moment in the model, we assumed that all muscles that could contribute to the moment are doing so with maximal activation. Experimentally, this may not be the case but it is not possible from this data to discern varying levels of activation to incorporate into the model.

3.3. Simulations

Trunk and lower extremity simulated jogging kinematics are shown in Fig. 3 and simulated joint moments are shown in Fig. 4. These joint angles and moments compare well to those measured experimentally in the literature (Brown et al., 2014; Novacheck, 1998), as well as those previously reported using full-body musculoskeletal simulation models (Hamner et al., 2010). Fig. 4 compares trunk and lower extremity (LE) joint moments during jogging simulated by Hamner et al. (2010) to the moments simulated using the FBLS model. There is some variability between the data as data from two different subjects have been compared, but overall the simulated moments compare well. Additionally, it is important to note that Hamner's model had no degrees of freedom in the spine. Fig. 5 shows the experimentally collected EMG and simulated activations. Generally, the LE muscle activations tend to compare well to EMG measured in this study and EMG reported during jogging in the literature (Cappellini et al., 2006), while some of the trunk muscles compare better than others. There may be more variability in trunk muscle activation than LE muscle activation during jogging because the trunk muscles primarily act as stabilizers during running and produce forces considerably lower in magnitude. Additionally, some discrepancies between EMG and simulated activations occur because SO is a frame-by-frame solver so anticipatory activations are not reflected in the

simulated activations. If anticipatory actions are of interest, Computed Muscle Control (CMC) should be used instead.

3.4. Limitations and conclusion

Limitations exist that should be considered when using this model. With 324 musculotendon actuators, the computational cost to create simulations with this model is higher than simpler models. This increased cost is a trade-off for a more physiologically accurate model. Additionally, spinal curvature in the FBLS model was not subject-specific. Future studies should consider using imaging techniques to accomplish this (Zhou et al., 2000), as spinal curvature has been shown to affect vertebral load magnitudes (Bruno et al., 2012).

The model is not yet suited for CMC or Forward Dynamics. This is likely because the maximum force property of some muscles were altered (described in Supplemental material Section 1.2) while the passive muscle property remained the same. The simulation results presented here are not affected by this discrepancy since the SO algorithm excludes the passive muscle force when calculating instantaneous muscle forces (Hicks and Dembia, 2014). CMC does not exclude passive muscle forces, so increasing F_0^m without also adjusting the passive muscle force property will lead to high passive muscle forces in the model (Thelen and Anderson, 2006). SO has been shown to predict muscle forces during walking and running that are comparable to those using CMC (Lin et al., 2012), and SO is considered more robust and computationally efficient than CMC (Mokhtarzadeh et al., 2014). Therefore, SO remains a valuable tool to investigate the behavior of muscle forces and activations during dynamic tasks.

While some trunk EMG was collected in this study, it was limited. EMG was not collected for some of the trunk muscles in the FBLS model (LD, QL, PS, MF) to compare with the estimated activations. Future studies should consider using more surface and
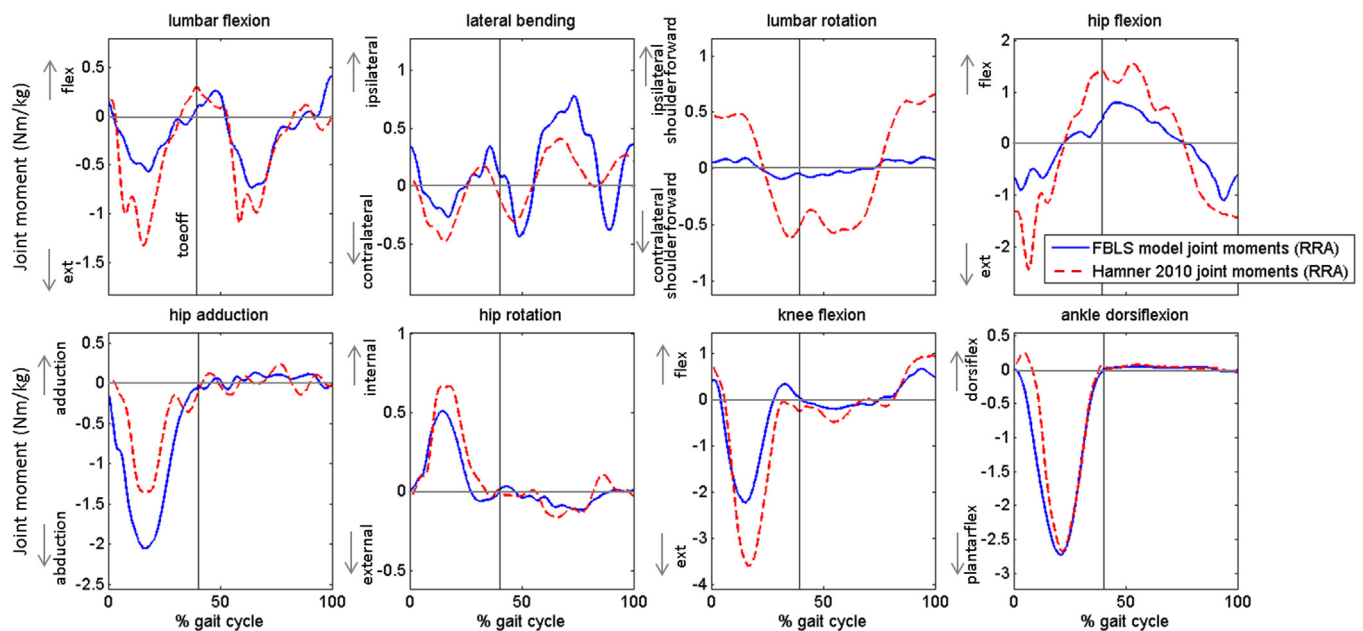
Fig. 4. Trunk and lower extremity (LE) joint moments during jogging simulated by Hamner et al. (2010) and using the FBLS model. Note the two studies simulate different subjects with different kinematics. Abbreviations: extension (ext), flexion (flex), plantarflexion (plantarflex), dorsiflexion (dorsiflex). The direction of lateral bending and lumbar rotation is with reference to the stance leg.
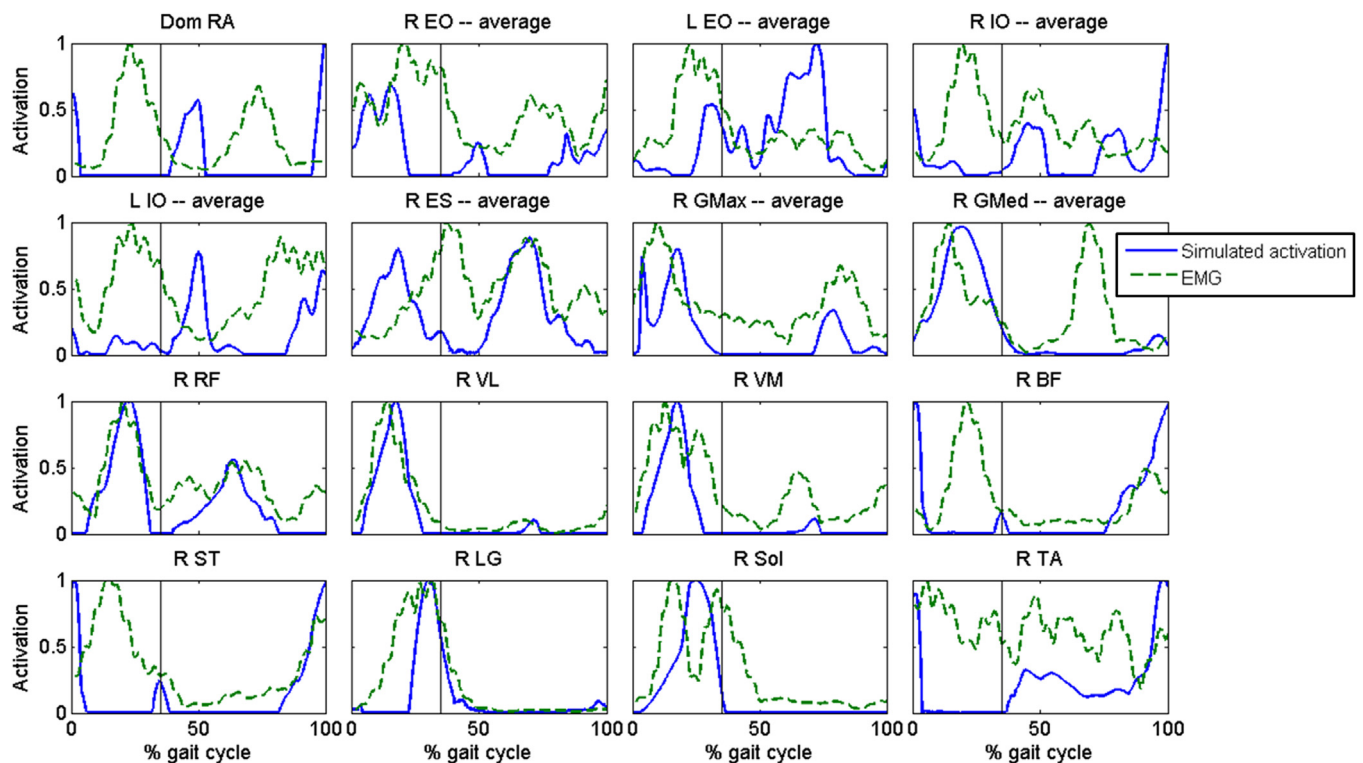
Fig. 5. EMG for all collected muscles (dashed line) compared to model activations calculated in OpenSim (solid line) through Static Optimization. The black vertical line represents toe-off. For simulated activations, the average activation for a muscle group modeled as multiple fascicles is reported, as noted.

fine-wire EMG on the trunk to further validate upper body muscle activations and force estimates in this model.

An OpenSim full-body musculoskeletal model was developed with detailed trunk musculature and degrees of freedom in the lumbar spine. The FBLS model is the first OpenSim model, to the best of the authors' knowledge to combine a complex model of the spine, involving detailed trunk musculature and degrees of freedom, with a well-established OpenSim lower extremity model. Future studies may explore integrating models of the spine that incorporate even higher complexity than the one used in this study (Bruno et al., 2015; de Zee et al., 2007). The FBLS model will be made freely available (https://simtk.org/home/fullbodylumbar) for others to perform additional analyses and develop simulations investigating full-body dynamics and contributions of the trunk muscles to dynamic tasks.

Conflict of interest statement

None.

Acknowledgments

Appendix A. Supplementary material

Supplementary data associated with this article can be found in the online version at http://dx.doi.org/10.1016/j.jbiomech.2016.02.046.

References

Arnold, E.M., Hamner, S.R., Seth, A., Millard, M., Delp, S.L., 2013. How muscle fiber lengths and velocities affect muscle force generation as humans walk and run at different speeds. J. Exp. Biol. 216, 2150–2160.

Arnold, E.M., Ward, S.R., Lieber, R.L., Delp, S.L., 2010. A model of the lower limb for analysis of human movement. Ann. Biomed. Eng. 38, 269–279.

Brown, T., O'Donovan, M., Hasselquist, L., Corner, B., Schiffman, J., 2014. Body borne loads impact walk-to-run and running biomechanics. Gait Posture 40, 237–242.

Bruno, A.G., Anderson, D.E., D'Agostino, J., Bouxsein, M.L., 2012. The effect of thoracic kyphosis and sagittal plane alignment on vertebral compressive loading. J. Bone Miner. Res. 27, 2144–2151.

Bruno, A.G., Bouxsein, M.L., Anderson, D.E., 2015. Development and validation of a musculoskeletal model of the fully articulated thoracolumbar spine and rib cage. J. Biomech. Eng. 137, 081003.

Cappellini, G., Ivanenko, Y.P., Poppele, R.E., Lacquaniti, F., 2006. Motor patterns in human walking and running. J. Neurophysiol. 95, 3426–3437.

Caruthers, E., Thompson, J.A., Schmitt, L.C., Best, T.M., Chaudhari, A.M.W., Siston, R.A., 2013. Individual muscle forces during a sit to stand transfer. In: Proceedings of the Annual Meeting of the American Society of Biomechanics, Omaha, NE.

Chaudhari, A.W., Jamison, S., Best, T., 2012. Proximal risk factors for ACL Injury: role of core stability. In: Noyes, F.R., Barber-Westin, S. (Eds.), ACL Injuries in the Female Athlete. Springer, Berlin, Heidelberg, pp. 169–183.

Christophy, M., Faruk Senan, N.A., Lotz, J., O'Reilly, O., 2012. A musculoskeletal model for the lumbar spine. Biomech. Model. Mechanobiol. 11, 19–34.

de Zee, M., Hansen, L., Wong, C., Rasmussen, J., Simonsen, E.B., 2007. A generic detailed rigid-body lumbar spine model. J. Biomech. 40, 1219–1227.

Delp, S., Anderson, F., Arnold, A., Loan, P., Habib, A., John, C., 2007. OpemSim: open-source software to create and analyze dynamic simulations of movement. IEEE Trans. Biomed. Eng. 54, 1940–1950.

Ferber, R., Bolgla, L., Earl-Boehm, J.E., Emery, C., Hamstra-Wright, K., 2015. Strengthening of the hip and core versus knee muscles for the treatment of patellofemoral pain: a multicenter randomized controlled trial. J. Athl. Train. 50, 366–377.

Hamner, S., Seth, A., Delp, S., 2010. Muscle contributions to propulsion and support during running. J. Biomech. 43, 2709–2716.

Hicks, J., Dembia, C., 2014. How Static Optimization Works.

Hicks, J.L., Uchida, T.K., Seth, A., Rajagopal, A., Delp, S.L., 2015. Is my model good enough? Best practices for verification and validation of musculoskeletal models and simulations of movement. J. Biomech. Eng., 137.

Holzbaur, K.R., Murray, W.M., Delp, S.L., 2005. A model of the upper extremity for simulating musculoskeletal surgery and analyzing neuromuscular control. Ann. Biomed. Eng. 33, 829–840.

Jamison, S.T., McNally, M.P., Schmitt, L.C., Chaudhari, A.M., 2013. The effects of core muscle activation on dynamic trunk position and knee abduction moments: implications for ACL injury. J. Biomech. 46, 2236–2241.

Jamison, S.T., McNeilan, R.J., Young, G.S., Givens, D.L., Best, T.M., Chaudhari, A.M., 2012. Randomized controlled trial of the effects of a trunk stabilization program on trunk control and knee loading. Med. Sci. Sports Exerc. 44, 1924–1934.

Jorgensen, M.J., Marras, W.S., Granata, K.P., Wiand, J.W., 2001. MRI-derived moment-arms of the female and male spine loading muscles. Clin. Biomech. 16, 182–193.

Keller, T.S., Roy, A.L., 2002. Posture-dependent isometric trunk extension and flexion strength in normal male and female subjects. J. Spinal Disord. Tech. 15, 312–318.

Khalaf, K.A., Parnianpour, M., Sparto, P.J., Simon, S.R., 1997. Modeling of functional trunk muscle performance: interfacing ergonomics and spine rehabilitation in response to the ADA. J. Rehabil. Res. Dev. 34, 459–469.

Kibler, W., Press, J., Sciascia, A., 2006. The role of core stability in athletic function. Sports Med. 36, 189–198.

Kumar, S., Dufresne, R.M., Van Schoor, T., 1995. Human trunk strength profile in lateral flexion and axial rotation. Spine 20, 169–177 (Phila Pa 1976).

Lin, Y.C., Dorn, T.W., Schache, A.G., Pandy, M.G., 2012. Comparison of different methods for estimating muscle forces in human movement. Proc. Inst. Mech. Eng. H 226, 103–112.

McGill, S., 2010. Core training: evidence translating to better performance and injury prevention. Strength Cond. J. 32, 33–46.

McGill, S., Juker, D., Kropf, P., 1996. Appropriately placed surface EMG electrodes reflect deep muscle activity (psoas, quadratus lumborum, abdominal wall) in the lumbar spine. J. Biomech. 29, 1503–1507.

Mokhtarzadeh, H., Perraton, L., Fok, L., Munoz, M.A., Clark, R., Pivonka, P., Bryant, A.L., 2014. A comparison of optimisation methods and knee joint degrees of freedom on muscle force predictions during single-leg hop landings. J. Biomech. 47, 2863–2868.

Novacheck, T.F., 1998. The biomechanics of running. Gait Posture 7, 77–95.

Thelen, D.G., Anderson, F.C., 2006. Using computed muscle control to generate forward dynamic simulations of human walking from experimental data. J. Biomech. 39, 1107–1115.

Willson, J., Dougherty, C., Ireland, M., Davis, I., 2005. Core stability and its relationship to lower extremity function and injury. J. Am. Acad. Orthop. Surg. 13, 316–325.

Zhou, S.H., McCarthy, I.D., McGregor, A.H., Coombs, R.R., Hughes, S.P., 2000. Geometrical dimensions of the lower lumbar vertebrae–analysis of data from digitised CT images. Eur. Spine J. 9, 242–248.